

We are IntechOpen, the world's leading publisher of Open Access books Built by scientists, for scientists

6,900

Open access books available

186,000

International authors and editors

200M

Downloads

Our authors are among the

154

Countries delivered to

TOP 1%

most cited scientists

12.2%

Contributors from top 500 universities



WEB OF SCIENCE™

Selection of our books indexed in the Book Citation Index
in Web of Science™ Core Collection (BKCI)

Interested in publishing with us?
Contact book.department@intechopen.com

Numbers displayed above are based on latest data collected.
For more information visit www.intechopen.com



Sidelobe Nulling by Optimizing Selected Elements in the Linear and Planar Arrays

Jafar Ramadhan Mohammed and Khalil H. Sayidmarie

Abstract

Currently, there are significant interests in the antenna arrays that are composed of a large number of elements controlled by an appropriate optimizer for the next generation of wireless communication systems, where the massive multiple-inputs multiple-outputs (MIMO) systems are expected to play a major role in such systems. On the other hand, the interfering signals which are expected to rise dramatically in these applications due to the crowded spectrum represent a real challenging issue that limits and causes great degradation in their performances. To achieve an optimum performance, these antenna arrays should be optimized and designed to have maximum gain, narrow beam width, and very low sidelobes or deep nulls. Toward achieving this goal, the overall array performance can be either electronically controlling the design parameters, such as amplitude and/or phase excitations of the individual elements, or mechanically controlling the element positions. This chapter discusses techniques proposed for sidelobe nulling by optimizing the excitations and positions of selected elements in the linear and planar arrays.

Keywords: antenna arrays, array pattern synthesis, null steering, sidelobe reduction, optimization algorithms

1. Introduction

Antenna arrays can be designed to reconfigure their radiation characteristics either by electronically controlling the amplitude and/or phase excitations of the array elements or by mechanically controlling the separation distances between the array elements. Accordingly, the null steering methods are generally divided into two main categories: electronic null steering and mechanical null steering. Each of them has its own advantages and disadvantages as will be shown in the following sections.

Generally, large antenna arrays are characterized by very high gains and narrow main beams. Thus, they are widely used in many applications including satellites, radio telescopes, communication systems, radar, sonar, and many other systems including future fifth generation (5G) wireless communication systems. The performances of these systems may degrade severely under the presence of interfering signals and/or ground clutter, which are unavoidable in such applications. Therefore, it is highly desirable to suppress, or at least reduce, the sidelobes into which the interfering signals are coming. This means that the shape of the radiation

pattern of such antenna arrays can be reconfigured to have maximum directive gain in the direction of its main beam and low sidelobes or deep nulls toward other unwanted directions.

In the literature, several strategies have been described to reshape the array radiation pattern. Among them, electronic phased arrays or more specifically beam forming has received considerable attention [1–3]. However, most of the adaptive algorithms that were used in such type of antennas are time-consuming because they involve a large number of iterations and they are not able to provide global optimum solutions. Reconfiguration of the array pattern with prescribed sidelobe structure mask can be also achieved by means of the global optimization approaches. The proposed approaches were genetic algorithm [4, 5], particle swarm optimization [6, 7], simulated annealing [8, 9], ant colony optimization [10], differential evolution algorithm [11], firefly algorithm [12], and some other methods [13], where the amplitude and/or phase of the elements excitations are the optimization parameters.

Apart from the aforementioned approaches, new directions in antenna array pattern reconfiguration have been proposed based on either adding a small number of extra elements on each side of the linear array [14–16], or by reusing the side (or end) elements of the linear arrays [17] or planar arrays [18, 19]. In these papers, the calculations that were required to find the values of the amplitude and phase excitations of the side elements basically relied on simple mathematical formulations and none of the optimization algorithms were used. Thus, the solutions were not optimum and there was a necessary need to search for an optimum solution for such an important scenario. Therefore, instead of a simple analytical method that was presented in [17], a more powerful method based on the genetic algorithm was proposed to find the optimal values of the amplitude and phase excitations for those electronically controllable edge elements with less computational time [20]. The method presented in [20] is further extended to obtain multiple wide nulls by properly selecting and optimizing the most effective elements in the array [21]. Wide nulls were also obtained by turning off some selected elements in the uniformly spaced linear arrays by means of binary genetic algorithm [22]. In all of those previous works, the null steering was performed electronically by controlling the amplitude and phase excitations of the array elements.

On the other hand, the mechanical null steering methods that are based on the controlling of the separation distance between the array elements were considered as an alternative and competitive solution to the electronic counterpart [23–25]. In [26], the author proved that the mechanical null steering made better patterns when compared with the electronic counterpart [20], by mechanically controlling the positions of the extreme elements while leaving all the electronic excitations including the edge elements constant.

The chapter is organized as follows: Section 2 provides a theoretical overview about electronic null steering including fully and partially controlled array elements. It also contains the sensitivity analysis of the generated nulls as well as how much the nulling is robust with respect to variations in the reconfigured amplitude and phase excitations. Section 3 provides a theoretical overview of a mechanical null steering including fully nonuniform spaced arrays and the proposed solution. It also explains the implementation strategies of the aforementioned technologies.

2. Electronic null steering methods

This technique involves the modification of amplitude and/or phase excitations of an N -element array. The amplitude and/or phase excitations of these array

elements should be specifically selected through an appropriate control system that is connected to each of the array elements. Clearly, for such electronic null steering strategy and for N elements linear array, we need N variable attenuators and N variable phase shifters for the feeding network. This results in a very complex feeding network especially for a large number of elements which, of course, becomes expensive and may be impractical. Therefore, a less costly and simpler system for reducing the effect of interfering signals is needed. In this section, a simple technique for sidelobe nulling over a wide angular region in the linear arrays is introduced, where only the electronic excitations of the two side elements of the array were needed to be controllable while maintaining the same performance of interference suppression. Thus, the feeding network of the proposed linear array contains, in most designs, only two phase shifters and one attenuator.

2.1 Linear array

Consider a linear array of N isotropic elements which are mechanically fixed by selecting the separation distance between the array elements to be uniform at a constant value d . These elements are symmetrically disposed with respect to the origin along the x -axis and suppose that a harmonic plane wave with wavelength λ is incident from direction θ and propagates across the array. The I signal outputs from the array elements are weighted by the amplitude excitation coefficients A_n and phase excitation coefficients P_n then summed to give the linear array output. The sidelobe nulling was achieved by properly adjusting the values of the attenuators and phase shifters that are connected to each element.

2.1.1 Single null

This subsection presents an efficient method for controlling the amplitude and phase excitations of the end elements by means of global optimization algorithms such as genetic algorithm or particle swarm optimization to generate a sector sidelobe nulling in the linear arrays without any reduction in the array gain [20]. To maintain the gain of the designed array and also to increase the convergence rate of the used optimization algorithms, some constraints on the searching spaces are included.

2.1.2 The electronic single null steering method

The structure of the electronically null steering array, with controlled amplitudes A_1 and A_N as well as controlled phases P_1 and P_N for the first and the last elements in a linear array is shown in **Figure 1** [20]. The amplitudes and phases of the edge-element excitations can be considered as either symmetric or asymmetric excitation. Note that the proposed array under the asymmetric excitation will have 4 degrees of freedom, while for the symmetric case it will have only 2 degrees of freedom. These numbers are also true when considering the optimization parameters. The far-field pattern of the electronically null steering array with controlled amplitude and phase excitations, assuming even number of elements, can be written as [20]:

$$AF(u) = \underbrace{\sum_{n=2}^{N/2} \cos\left(n - \frac{1}{2}\right)\psi}_{N-2 \text{ uniform array}} + \underbrace{A_1 e^{j\left(\frac{N-1}{2}\right)\psi + P_1} + A_N e^{-j\left(\frac{N-1}{2}\right)\psi + P_N}}_{\text{Edge elements alone}} \quad (1)$$

where $\psi = (2\pi d/\lambda)u + \beta$. Here, $u = \sin(\theta)$, and θ is the observation angle from the array normal, d is the element spacing which is selected to be fixed at $d = \lambda/2$ for all array elements, and β is the phase shift required to steer the angle of the main beam. Knowing the direction of the interfering signals, u_i , $i = 1, 2, \dots, I$ (where I is the total number of interfering signals), and substituting for $AF(u_i) = 0$ according to the interference suppression condition, the nulls directions u_i can be computed from (1).

For asymmetric array, note that the above equation cannot be solved analytically using the method introduced in [17] since it is a function of four unknown parameters, i.e., A_1 , A_N , P_1 , and P_N . On the other hand, the optimal values of these four parameters, subject to some constraints, can be easily found using any global optimization algorithm such as genetic algorithm or particle swarm optimization (PSO), as can be seen in the following subsection [20]. As mentioned earlier, the main constraints that are applied during the optimization process are the depth of the generated nulls and the main beam shape preservation. Moreover, some constraints on the optimization parameters are also considered, where the minimum and maximum values of the optimized amplitudes A_1 and A_N are set to 0 and 1, respectively, and for optimized phases P_1 and P_N are set to $-\pi/2$ and $\pi/2$, respectively [20]. To show the effectiveness of the proposed method, it is applied to uniformly excited linear arrays as well as some nonuniformly excited linear arrays such as Dolph and Tayler arrays as can be seen in the following subsection [20].

2.1.3 The results

In order to show the advantages of the proposed array with controlled two edge elements, first the fully controlled array (i.e., the amplitude excitation of all array

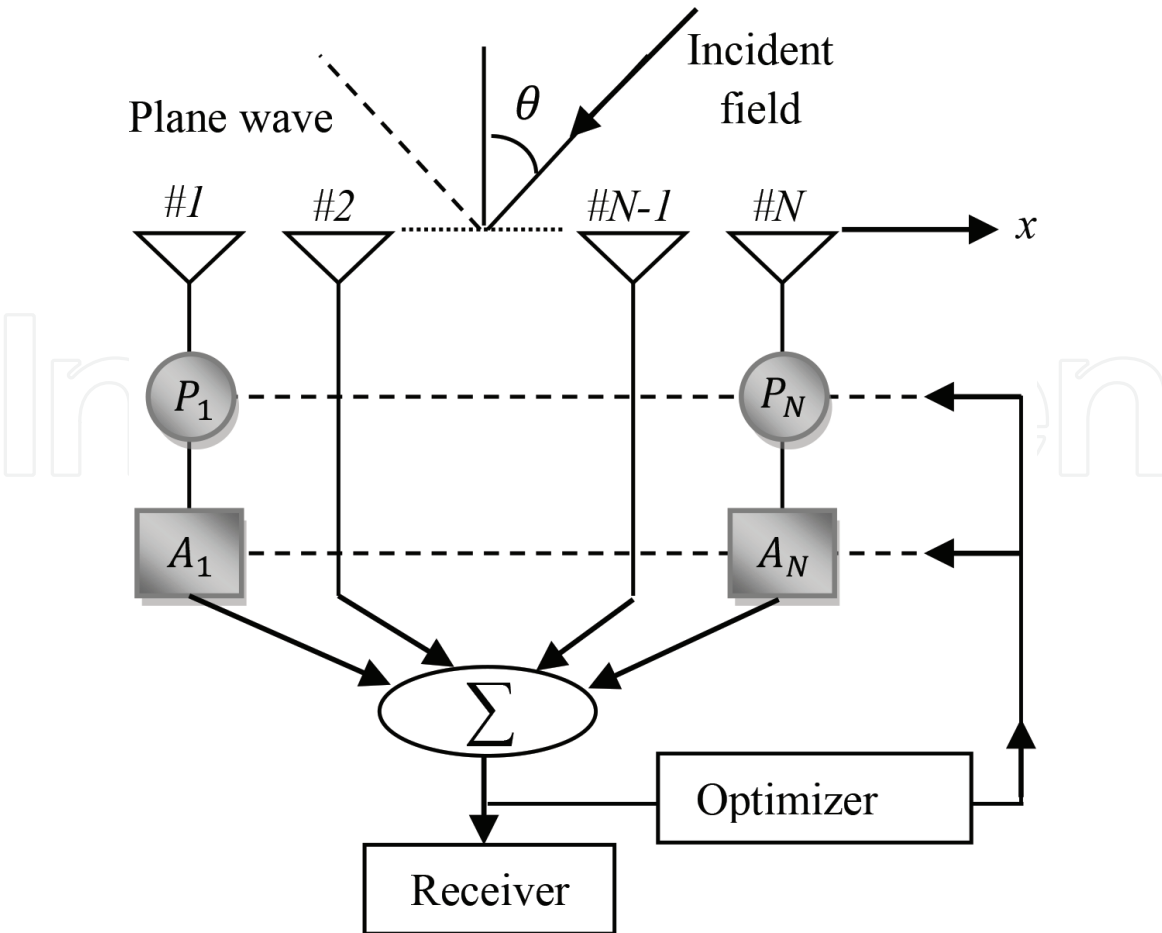


Figure 1.
Block diagram of the single wide null method [20].

elements are controlled including the two edge elements) is considered. In this example, the total number of array elements are chosen to be $N = 30$ elements, the amplitude excitation of the original array elements is chosen to be uniform and the phase excitation is set to zero. In this scenario, the genetic algorithm is used to optimize the amplitude excitations of all array elements while the phase excitations are left unchanged. The required sidelobe level was set at -40 dB. **Figure 2** shows the optimized array pattern along with the original uniform array pattern. It can be seen that the required sidelobe level is accurately achieved while the HPBW and FNBW have increased. The amplitude excitations of all array elements are greatly changed except a small number of the central elements. Moreover, the optimizer needs at least 250 iterations to converge.

For a fully controlled array, the number of degrees of freedom is quite enough to reduce the sidelobe level and at the same time to place the desired nulls, as shown in **Figure 3**. Here, as in the previous case, the required sidelobe level is chosen to be

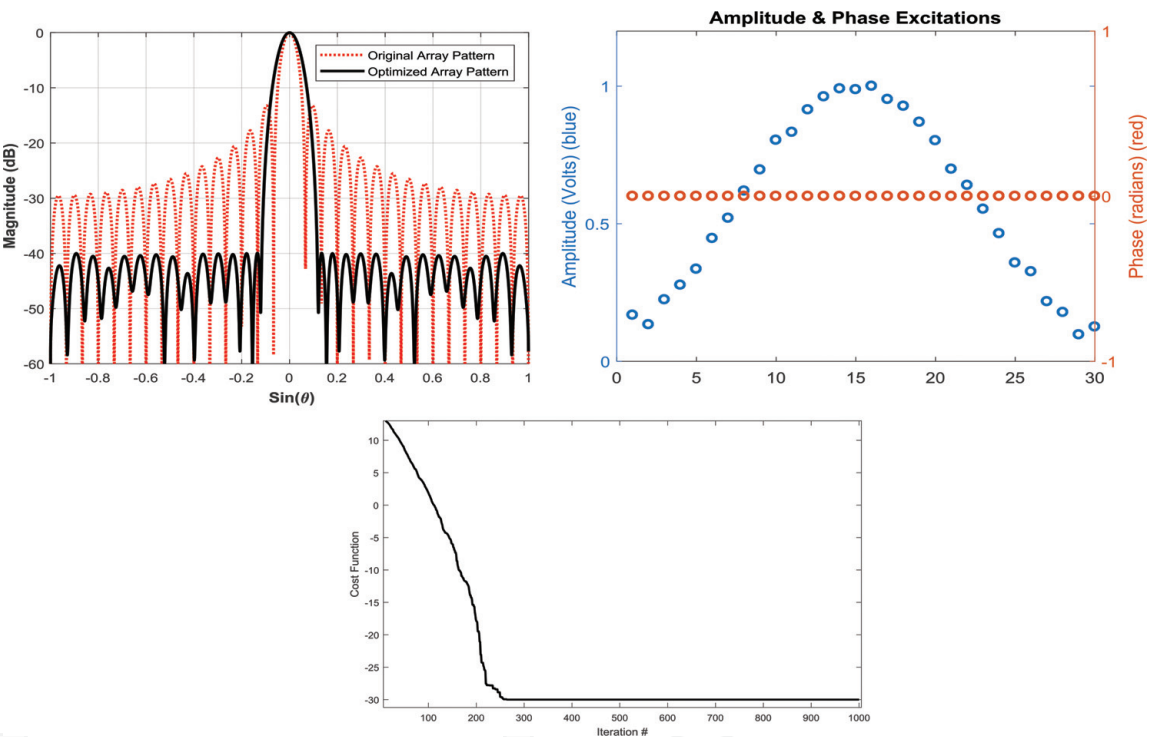


Figure 2.
Results for fully electronic null steering method for $N = 30$ and $SLL = -40$ dB.

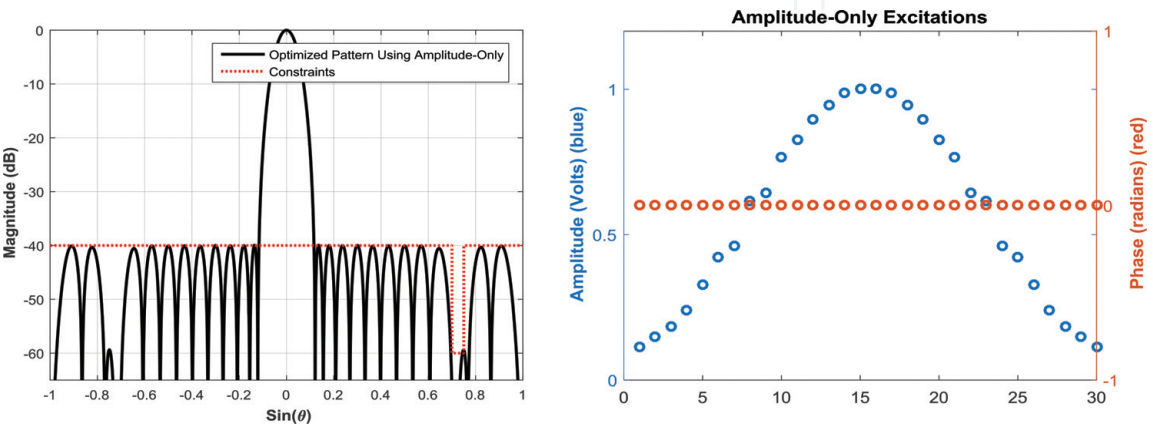


Figure 3.
Results for fully electronic null steering method with amplitude only control for $N = 30$, $SLL = -40$ dB, and a single wide null.

−40 dB and a single wide null centered at $u = 0.75$ (ranged from $u = 0.73$ to 0.77) is considered. Similar results are obtained when the amplitude and the phase excitations of the full elements are optimized are shown in **Figure 4**.

All of the above results show clearly that the required shape of the array pattern can be obtained only when precisely choosing the values of the attenuators. In practice, the attenuators are digital and they have a limited number of quantized levels. Thus, these required shapes are far or even impossible to get. Therefore, the arrays that are composed of a few controllable elements are very desirable in practice. In the next example, we consider an array of $N = 100$ elements and only the edge element are optimized by either the GA or PSO algorithm. Here, only a single wide null is required to be placed from $u = 0.4$ to 0.5 with depth −60 dB. Moreover, the original excitations of all array elements are assumed to be uniform. **Figure 5** shows the radiation patterns of the optimized arrays using GA and PSO along with the original uniform array pattern. This figure also shows the convergence rate of the optimizer under these two different algorithms.

It can be seen that the optimized arrays by GA and PSO are equally capable of achieving the required wide sidelobe nulling. The HPBW of the original uniform array, and the optimized array are 1.0084 and 1.0314° , respectively. For this case, the optimized values of A_1 , A_N , P_1 , and P_N using GA were found to be 0.8181 , 0.7313 , 52.2824 and -47.6185° , respectively; whereas, these value were found to be 0.7322 , 0.8179 , 47.7388 and -52.4027° for PSO design. The computational times for GA and PSO were found to be 0.15429 and 0.12667 min, respectively.

In **Figure 6**, the results of the proposed single null steering method is examined for $N = 30$ elements and the desired null is from $u = 0.7$ to 0.75 with a depth equal to −60 dB. This figure also shows the required amplitudes and phases of both the original and optimized arrays.

By comparing the results of **Figure 6** with those of **Figure 3** or **Figure 4**, it can be clearly seen that the proposed single null steering method requires only one attenuator and two phase shifters to realize the modified element excitations. However, the fully controlled array requires at least 30 attenuators and 30 phase shifters to realize the reconfigured amplitude and phase weights. This fully confirms the effectiveness of the proposed single null steering method.

Moreover, to show the generality of the proposed method, we extend it to the nonuniformly excited arrays such as Dolph and Taylor arrays. **Figures 7** and **8** show the radiation patterns of the Dolph and Taylor arrays ($N = 30$ elements, and $SLL = -40$ dB), where the excitations of the edge elements are optimized using GA for the purpose of generating sector sidelobe nulling with same width and depth as in the previous example.

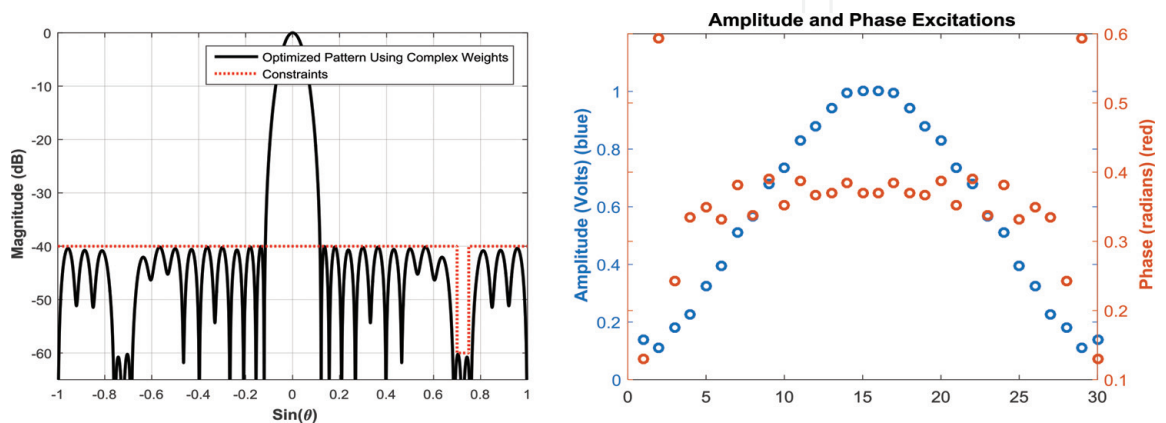


Figure 4. The results for fully electronic null steering method with amplitude and phase excitations for $N = 30$, $SLL = -40$ dB, and a single wide null.

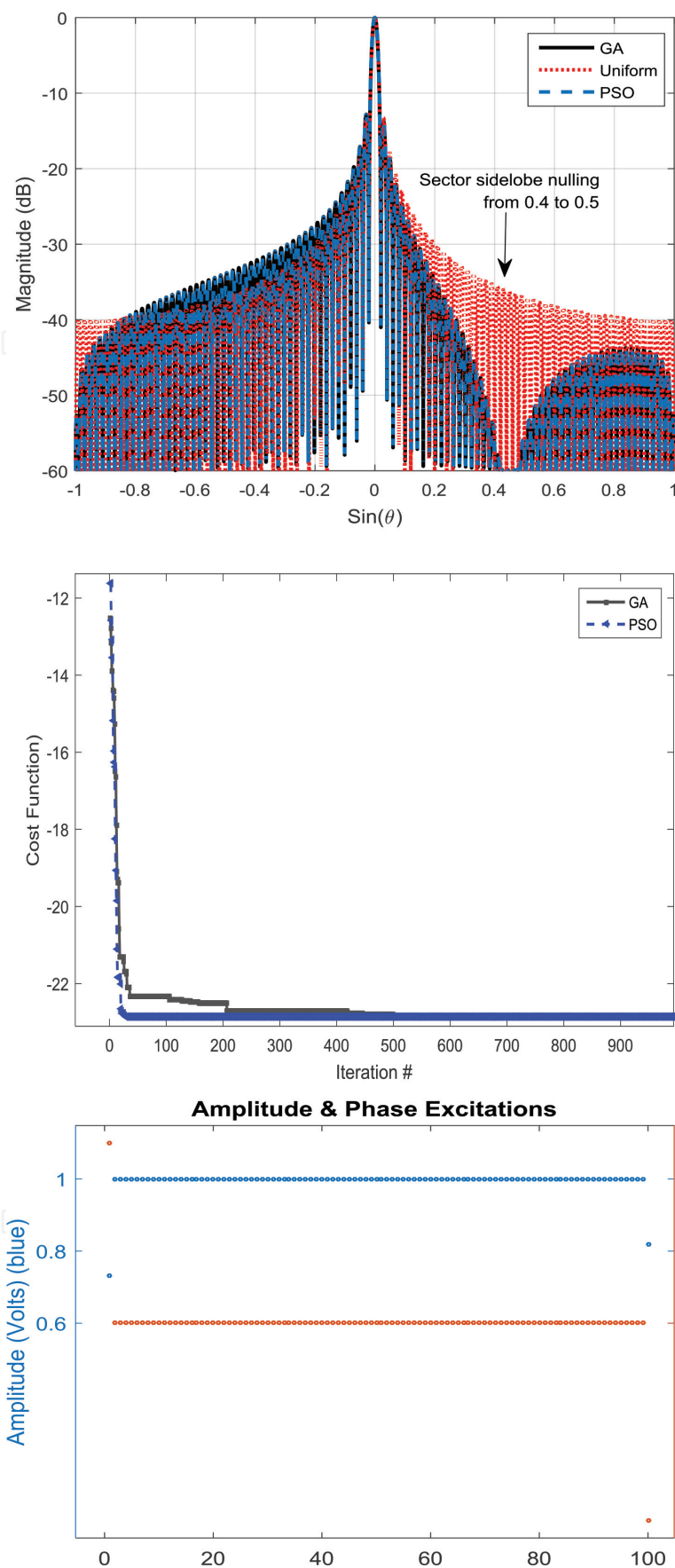


Figure 5.
The results for the proposed single null steering method for $N = 100$.

2.1.4 Multiple nulls

As we have shown in the previous subsection that a single wide null requires at least controlling the excitations of the two end elements in a linear array. In many

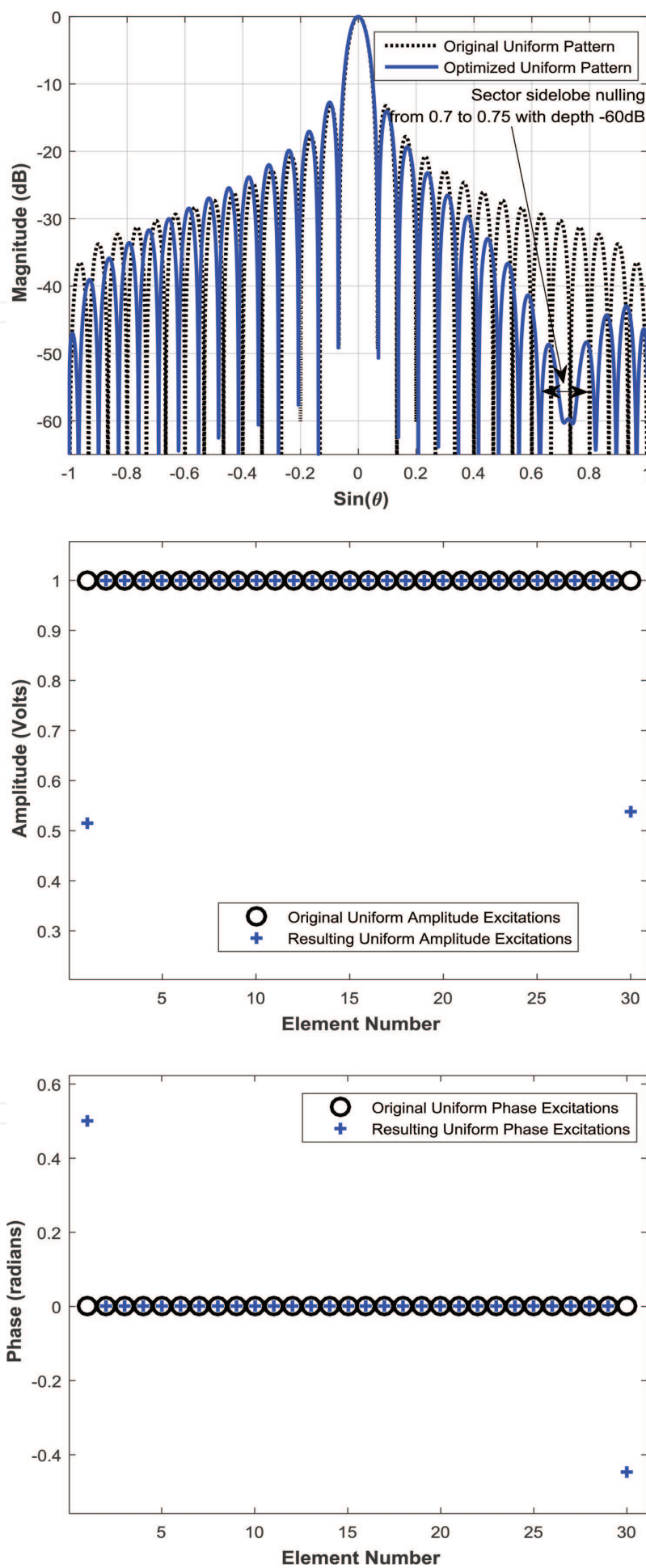


Figure 6.
The results for the proposed single null steering method for $N = 30$.

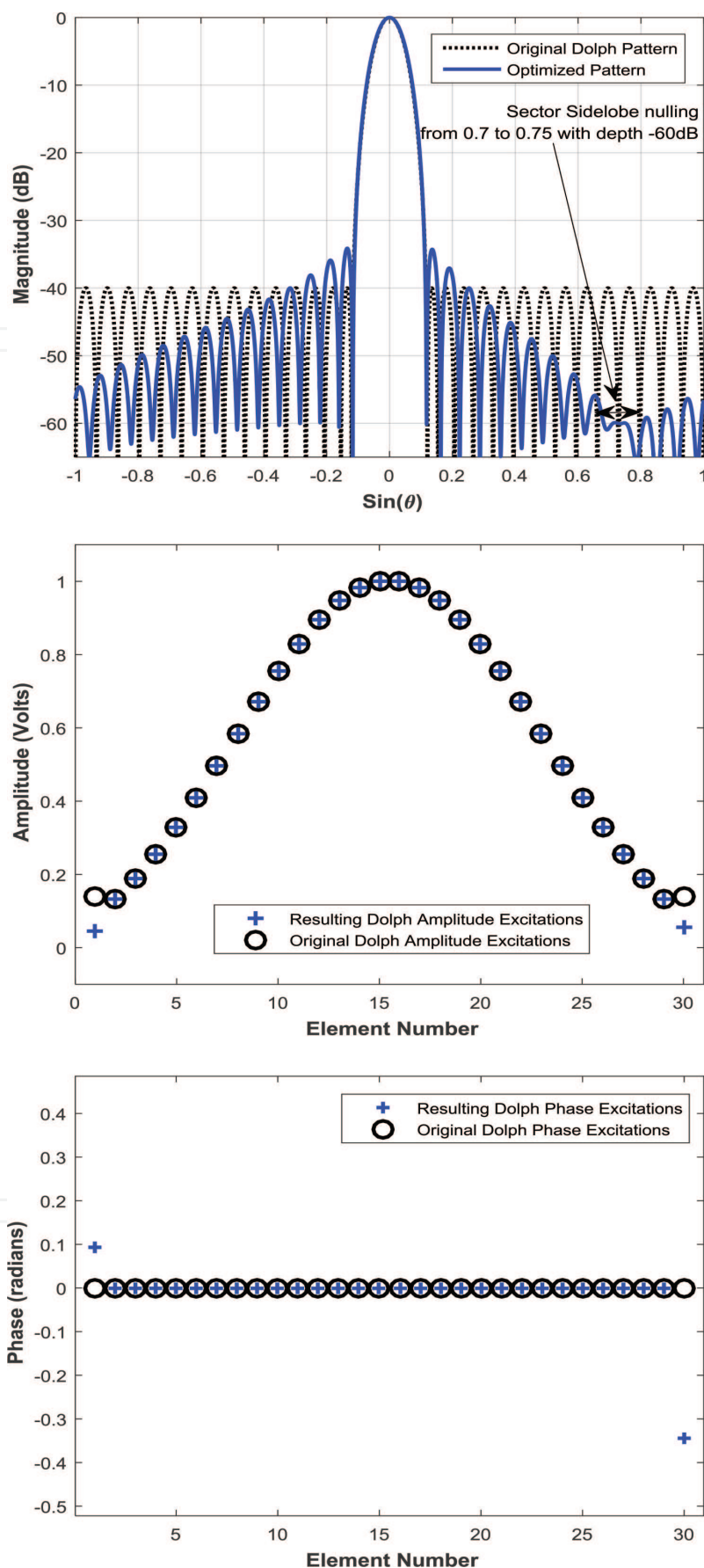


Figure 7.
Results for the proposed single null steering method for $N = 30$ and Dolph excitation.

applications with multi interference environment, it is desirable to generate multiple wide nulls in the radiation pattern; thus, a set of element excitations have to be modified. In this subsection, a subset of a small number of adjustable elements on

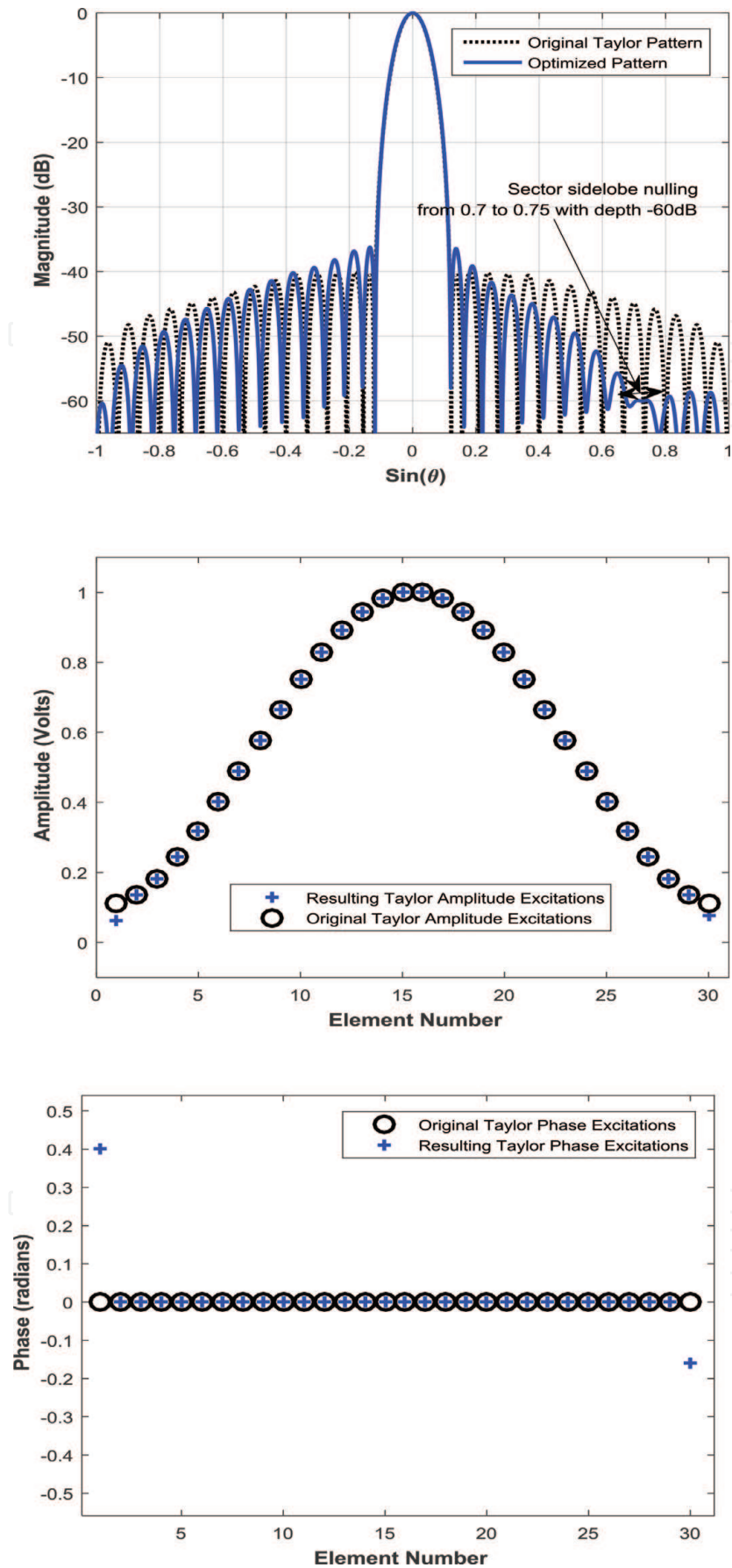


Figure 8.
Results for the proposed single null steering method for $N = 30$ and Taylor excitation.

both sides of the array is considered. Therefore, the far-field equation of the overall array is formulated as the summation of two independent array subsets. The first array subset is referred to as a uniform array, which contains the majority of the

array elements; whereas, the second array subset contains only a small number of the array elements that will be adjusted adaptively. The GA is used to optimize the amplitude and phase excitations of the second array subset elements [21].

2.1.4.1 The electronic multiple null steering method

Here in this subsection, the solution proposed in Section 2.1.2 is further extended to include which elements are to be optimized and to what extent. The small number of the selected elements should have an impact on the controllable nulls. Therefore, we examine three different selection strategies. The first strategy selects the most effective elements that are located on the extremes of the array; while in the second and third strategies, the selections consider the elements that are located at the center of the array or randomly chosen from the whole array elements [21]. The idea of the second strategy was employed in a sidelobe adaptive canceller system [27]. By adapting few elements at the center of the array, the system is capable to produce multiple nulls toward a number of interfering signals [27]. Experience with these three selection strategies showed that the first strategy provides best performance for interference suppression [21]. To apply the first strategy, first, consider an array of an even number of elements $2N$, with uniform amplitude excitations and mechanically fixed locations with uniform inter-element spacing d , symmetrically positioned about the origin (i.e., N elements are placed on each side of the origin). Assuming a subset of only $2M$ elements (out of the $2N$ -element array) is optimized to generate the required nulls at unwanted directions (i.e., M outer elements on each end of the array). The remaining $2N-2M$ elements are kept unchanged, i.e., having uniform amplitude and equal-phase excitations. The overall far-field pattern due to the $2N-2M$ uniformly excited array elements and the $2M$ adaptive array elements can be written as [21]:

$$AF(u) = \underbrace{2 \sum_{n=1}^{N-M} \cos \left[\frac{(2n-1)kdu}{2} \right]}_{2N-2M \text{ uniform array}} + \underbrace{\sum_{m=N-M+1}^N \left\{ A_{m_r} e^{j \left(\frac{(2m-1)kdu}{2} + P_{m_r} \right)} + A_{m_l} e^{-j \left(\frac{(2m-1)kdu}{2} + P_{m_l} \right)} \right\}}_{2M \text{ elements array}} \quad (2)$$

where $k = 2\pi/\lambda$. From (2), it can be noted that the amplitudes (A_{m_r} and A_{m_l} for right and left subset elements) and phases (P_{m_r} and P_{m_l} for right and left subset elements) of $2M$ adjustable elements array can be considered either symmetric or nonsymmetric (i.e., $A_{m_l} \neq A_{m_r}$ and $P_{m_l} \neq P_{m_r}$) like the earlier method. Also note that the $2M$ adjustable elements are selected from the extremes of the array and they play an important role in generating the required nulls. The structure of the interior $2N-2M$ uniformly excited array elements with adjustable amplitude and phase excitations of the outer M elements on each side of the array is shown in **Figure 9** [21].

2.1.4.2 The results

An original uniform linear array with $2N = 100$ elements located at fixed positions and having element separation equals to half the wavelength is considered. **Figure 10** shows the results obtained from the original uniform array and the optimized array patterns with four required wide nulls each of width $u = 0.05$ and depth = -60 dB. Five elements at each side of the linear array are used here as the elements to be controlled. To show the effectiveness of the proposed array with respect to the fully optimized array, the radiation pattern of the fully phase-only optimized array and its convergence speed are also included in **Figure 10**. It can be

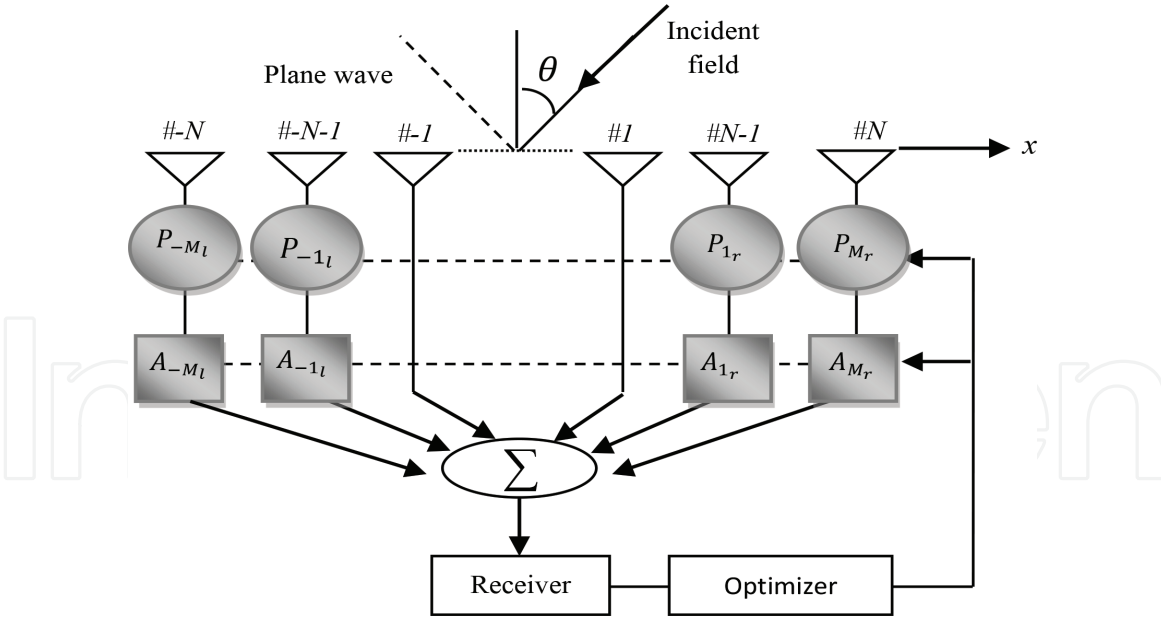


Figure 9.
Configuration of the multiple null steering method [21].

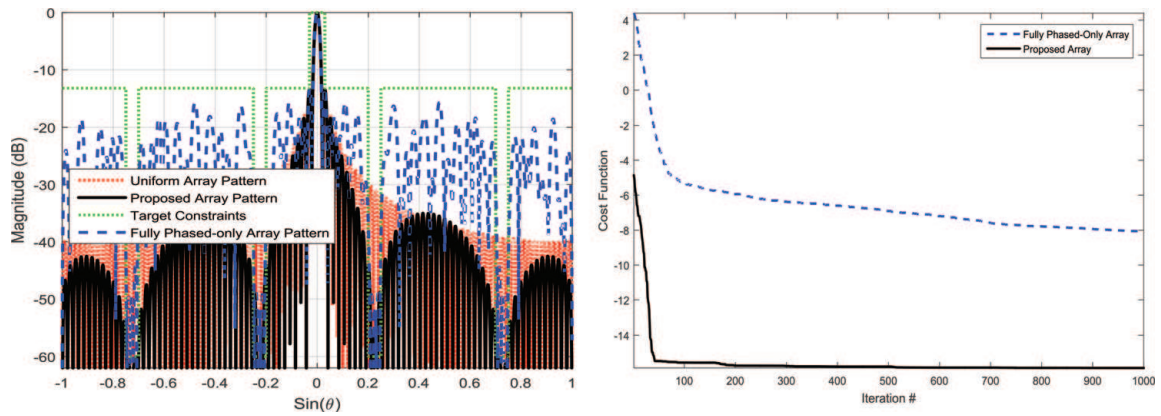


Figure 10.
Results of multiple wide null steering method.

seen that the proposed array with only 10 adjustable outer elements is capable of generating the required multi nulls at pre-specified depths and widths. The same performance is obtained with the fully phase-only optimized array but with an extra requirement of modifying the phases of 100 elements (i.e., more cost and more optimization parameters). The half power beam width of the fully uniform and the proposed arrays are 1.0085° and 1.0772° , respectively. Moreover, the proposed method converges much faster than the method of fully phased-only optimized array. The amplitude and phase excitations of the proposed and the fully phased-only optimized arrays are shown in **Figure 11**. From this figure, it can be seen that the required percentage of the perturbed element excitation represents only 10% of those needed for the fully phased-only optimized array. This drastically reduces the RF components of the feeding network and consequently the cost while maintaining the same performance of interference suppression.

2.2 Planar array

In this section, the selection process of the controllable elements is extended to the large planar arrays to reach the desired radiation pattern with a minimum

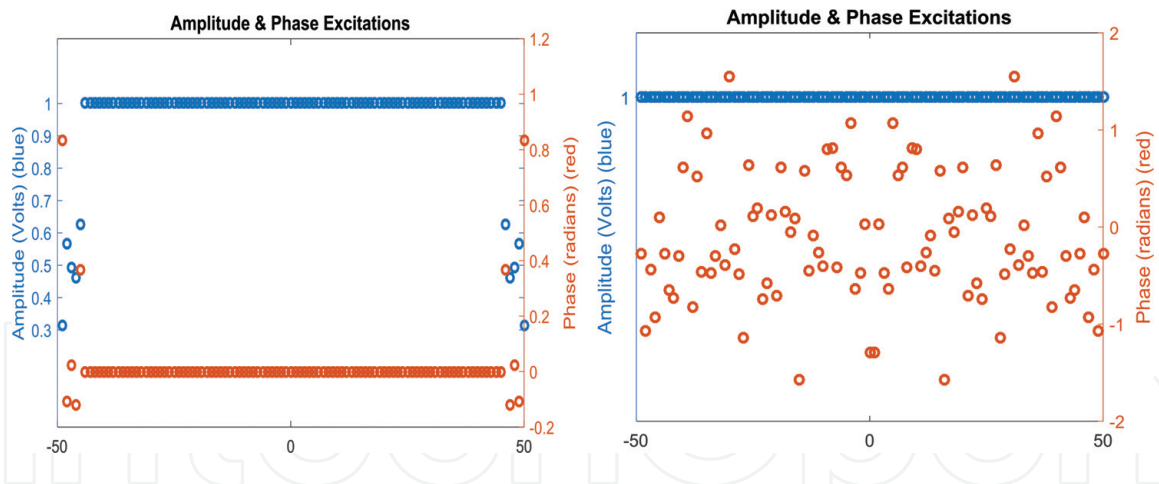


Figure 11.
 Amplitude and phase excitations of the proposed array and fully phase-only array.

number of adjustable elements, where the searching spaces are restricted to include only the elements on the array's perimeter [28]. The optimization was performed under some constraints to obtain the desired radiation characteristics such as narrower beamwidth, asymmetric low sidelobes, and controlled nulls in some pre-specified directions. Unlike the existing methods, in which all the array elements are changeable, the proposed planar array enjoys a faster convergence of the optimizer as its interior elements are fixed and the whole array keeps maintaining a good performance [28].

2.2.1 The electronic planar null steering method

Consider a rectangular planar array composed of N rows and M columns of isotropic elements with mechanically fixed inter-element spacing $d = \lambda/2$ in both x and y directions. The radiation pattern of such rectangular planar array can be written as [28]

$$AF(\theta, \phi) = \sum_{n=1}^N \sum_{m=1}^M w_{nm} e^{j \frac{2\pi d}{\lambda} [(n - \frac{N+1}{2})(\sin(\theta) \cos(\phi) - \beta_x) + (m - \frac{M+1}{2})(\sin(\theta) \sin(\phi) - \beta_y)]} \quad (3)$$

where θ is the elevation angle, ϕ is the azimuth angle, and $\beta_x = \sin(\theta_0) \cos(\phi_0)$, $\beta_y = \sin(\theta_0) \sin(\phi_0)$ are progressive phase shifts in x and y directions that are necessary to direct the mainbeam to the angle (θ_0, ϕ_0) , and w_{nm} is the complex weight of the (n, m) th element. Clearly, the array factor in (3) represents a fully controllable planar array in which all of its elements are adjustable and the resulting feeding network is a relatively complex system. Furthermore, to meet the required radiation characteristics, it is necessary to impose some constraints on the array weights which lead to an added complexity to the adaptive system. Thus, the necessity of controlling a small number of array elements arises especially with the practical implementation of large planar arrays or when faster adaptation is desirable.

In this work, the weights of the interior elements of the array (i.e., the central part having dimensions $(N - 2) \times (M - 2)$) are assumed to be constant, i.e., $w_{nm} = 1$, while the elements on the perimeter are only considered to be adjustable (or controllable) subject to some required constraints. Thus, the array factor of (3) can be rewritten as [28]

$$\begin{aligned}
 AF(\theta, \phi) = & \underbrace{\sum_{n=2}^{N-1} \sum_{m=2}^{M-1} e^{j \frac{2\pi d}{\lambda} \left(\left(n - \frac{N+1}{2} \right) (\sin(\theta) \cos(\phi) - \beta_x) + \left(m - \frac{M+1}{2} \right) (\sin(\theta) \sin(\phi) - \beta_y) \right)}}_{\text{interiorelements}} \\
 & + \underbrace{\sum_{m=1}^M (w_{1m} \{.\} + w_{Nm} \{.\}) + \sum_{n=2}^{N-1} (w_{n1} \{.\} + w_{nM} \{.\})}_{\text{Perimetelements}}
 \end{aligned} \tag{4}$$

where $\{.\}$ represents the exponential term as expressed in the first term of Eq. (3). The perimeter elements in the lower term of (4) are expressed as the sum of 2 rows and 2 columns. In the two rows, the value of n is set to $n = 1$ and $n = N$, while the value of m is allowed to change from 1 to M . In the two columns, the value of m is set to $m = 1$ and $m = M$, while the value of n is allowed to change from 2 to $M-1$ [28].

2.2.2 The results

In this subsection, a uniform planar array with $N = 6$ and $M = 6$ isotropic elements spaced by half a wavelength is considered. The required half power beamwidth (HPBW) of the proposed planar array pattern is chosen to be 17° , i.e., $\Omega_{BW} = 8.5^\circ$. Note that, for a uniformly excited planar array with size 6×6 elements the HPBW is also 17° . This means that the HPBW of the optimized array is constrained to be the same as that of the uniformly excited planar array.

Assume the direction of the desired signal is known, which is set to be 90° . The weights of the perimeter elements in the proposed planar array are optimized such that the corresponding radiation pattern has equal sidelobe level at -20 dB and two nulls at $\phi = -30^\circ, \theta = 80^\circ$ (i.e., $u_x = 0.852, u_y = -0.492$) and $\phi = 45^\circ, \theta = -70^\circ$ (i.e., $u_x = -0.664, u_y = -0.664$). **Figure 12** shows the radiation patterns of the original uniform planar array and the proposed array. It can be seen that the required sidelobe level and the desired null are efficiently accomplished by optimizing only the perimeter elements.

The corresponding complex weights (i.e., the magnitudes and the phases) of all elements in the proposed planar array are shown in **Figure 13**. It can be seen that only the magnitudes and the phases of the 20 perimeter elements are adjusted, whereas the 16 interior elements remain holding their uniform excitations.

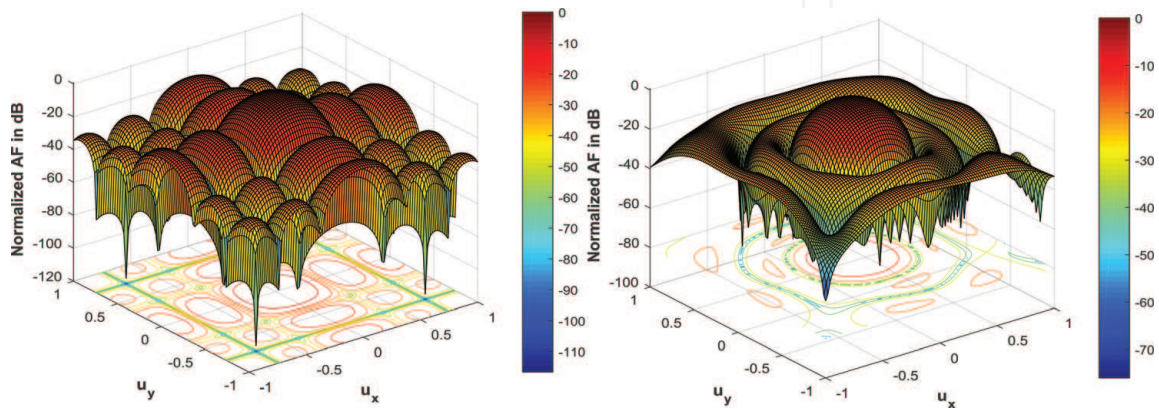


Figure 12. Optimized radiation pattern of the proposed planar array (right) and the uniformly excited planar array (left).

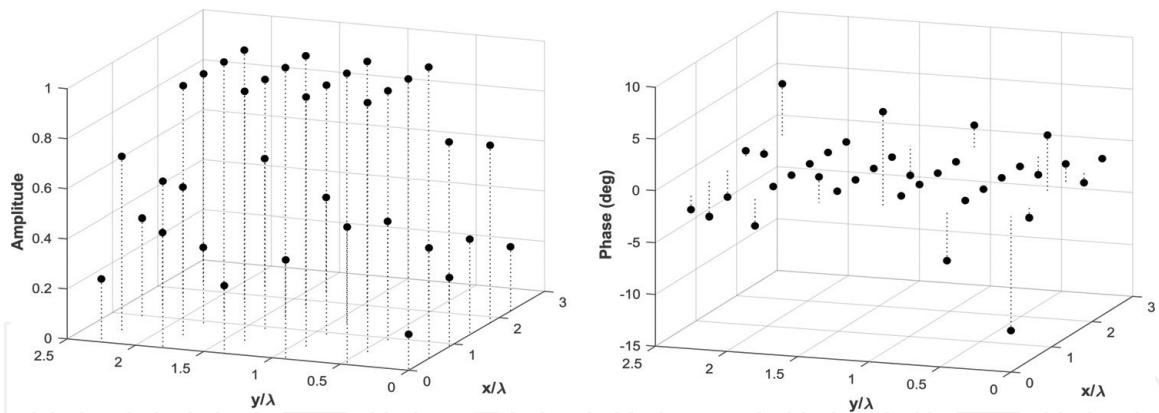


Figure 13.
 Amplitude and phase excitations of the proposed planar array pattern that is shown in Figure 12.

2.3 The sensitivity analysis

In this section, a realistic situation is investigated where the required element excitations in amplitude and phase cannot be realized exactly in practice, or when there is some fluctuation in the frequency of operation. The performance of the proposed optimization techniques and the null positions are investigated when there are some errors in the excitation of the array elements.

2.3.1 The effect of quantization levels on the generated nulls

In this section, the sensitivity analysis is concerned with how much the generated nulls are robust with respect to unavoidable variations of the reconfigured amplitude and phase weights due to the quantization errors that are associated with the used digital attenuators and/or digital phase shifters. The electronic null steering methods including the above-mentioned methods require phase shifters and attenuators that are digitally controlled. With such digital components, it is well-known that only a finite number of quantized values are available. For example, a one-bit digital phase shifter produces only two phase values of 0 and π , while a two-bit digital shifter can realize four phases of 0, $\pi/2$, π , and $3\pi/2$. Accordingly, with the use of discrete phase shifters and/or discrete attenuators, precise control over both amplitudes and phases of the adjustable elements is not possible. Therefore, unavoidable quantization error in the phase and/or amplitude excitations causes some modifications of the radiation pattern from the desired one. However, such performance degradations may be lesser in the proposed approaches than that in the fully optimized array elements where the number of the adjustable elements is small. **Figure 14** shows the sensitivity of the proposed multiple null steering method to various phase quantization levels. The effect is obvious on the sidelobe level and null depths.

The degradation in the optimized array pattern due to random errors in the phase and amplitude of the element excitations was investigated in [29]. Such errors can cause an elevation in the sidelobe level and changing the angular locations of the desired nulls. The simulation results showed that the nulls and the sidelobe level in the adaptive arrays are more sensitive to random errors in the element phase excitations as compared to amplitude excitations.

2.3.2 The effect of frequency fluctuation on the generated nulls

In this subsection, we assume that there is a fluctuation in the frequency of operation, or the system works on a certain band of frequencies around the center

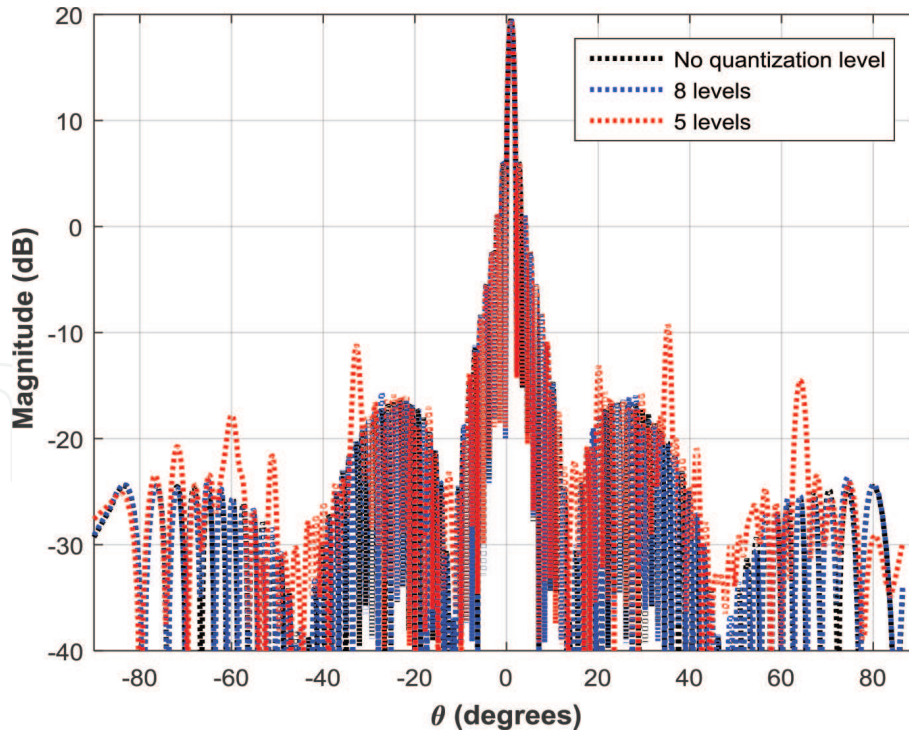


Figure 14.
Sensitivity of the proposed multiple null steering method to various phase quantization levels.

frequency. It is assumed that the element positions can be accurately fixed at the design frequency f_o , and element separation is fixed at $d = \lambda_o/2$, where λ_o is the free-space wavelength at the frequency f_o . In this case, the array factor of the uniformly excited equally spaced linear array can be found from [30] as:

$$AF(f, \theta) = \frac{\sin \left[\frac{Nf}{2f_o} \pi \sin(\theta) \right]}{\sin \left[\frac{1f}{2f_o} \pi \sin(\theta) \right]} \quad (5)$$

where f is instantaneous frequency, and f/f_o is the fluctuation or deviation ratio. From (5), the angle of the n^{th} null θ_n as a function of the frequency can be written as [30]:

$$\theta_n(f) = \sin^{-1} \left[\frac{f_o}{f} \left(\pm \frac{2n}{N} \right) \right] \quad (6)$$

A sample array of $N = 10$ elements working at an instantaneous frequency f and design frequency of $f_o = 3$ GHz is investigated here. **Figure 15**(left) shows the radiation patterns of the uniform array, plotted for frequencies higher than the design value $f_o = 3$ GHz. It can be seen that the angular location of the first null, in the uniform pattern is 11.54° , whereas this null is shifted to 9.871° when f is changed from 3 to 3.5 GHz. The figure also shows that, as the frequency departs from the design value $f_o = 3$ GHz, the nulls move toward main beam resulting in an increased magnitude at the original directions of the nulls. **Figure 15**(right) shows the radiation patterns of the same array plotted for frequencies lower than the design value f_o . It can be seen that the angular location of the first null is shifted from 11.54 to 13.8° when f is changed from 3 to 2.5 GHz; whereas, the forth null is shifted from 53.33 to 74.0° when f is changed from 3 to 2.5 GHz. The figure shows that, for frequencies lower than the design value $f_o = 3$ GHz, the nulls move far from the main beam resulting in an increased magnitude at the original directions of the

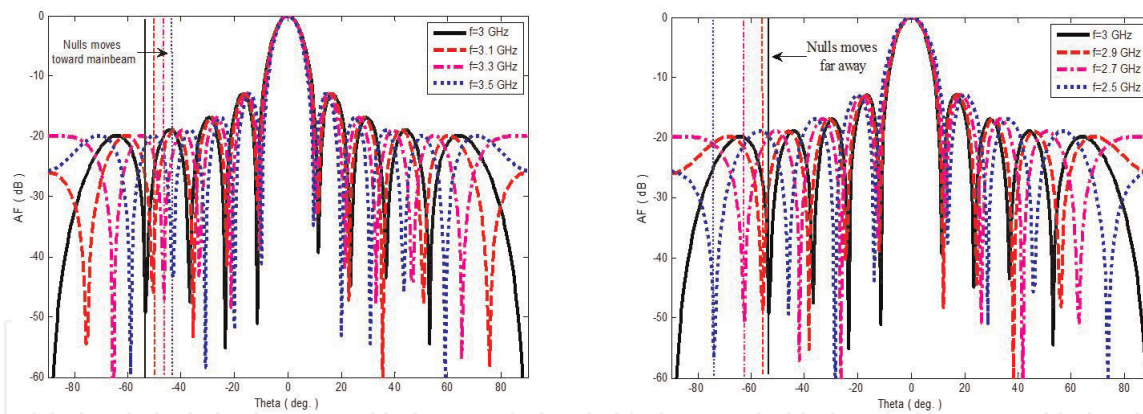


Figure 15.
 The effect of the frequency changes on the null positions for $N = 10$ elements, and design frequency $f_0 = 3\text{GHz}$ [30].

nulls. Generally, it is noticed that the nulls positions are sensitive to frequency changes. The sensitivity of the null angle θ_n to frequency can be found from Eq. (6) as [30]:

$$\frac{d\theta_n}{df} = \frac{1}{\sqrt{1 - \left(\frac{2nf_0}{Nf}\right)^2}} \quad (7)$$

The above relation shows that the sensitivity is a nonlinear function of the frequency deviation. This nonlinearity can be obviously noticed by comparing **Figure 15**(left) and (right), where a 0.5 GHz change in frequency produces different shifts in the null positions depending if the change is positive or negative. It has been found that a $\pm 16.7\%$ changes in the frequency result in a shift of 2.26 and 1.67°, respectively, for the first null position. In this example, a relatively large frequency span of 1 GHz has produced null movement of only 3.89°.

3. Mechanical null steering methods

As we have shown in the previous section, the practical implementation of the feeding network in the electronically null steering methods is a real challenging issue, especially when dealing with large arrays. To solve this problem, many researchers, for example, see [22–26], proposed to mechanically control the spacing between the array elements instead of electronically controlling the amplitude and/or phase excitations to achieve the required null steering. However, in practice, these fully nonuniform spaced arrays have also some disadvantages and difficulties to build. These difficulties may especially arise when dealing with movable or unknown interfering directions where in such a case it is required to continuously readjust the element positions to achieve the desired null steering. This means that the mechanical position of all elements in an array needs repeatedly to be recalculated and accordingly the whole array elements need to be removed for each specific interfering direction. In such methods of mechanically nonuniform spaced arrays, the simplest way to change the position of the array elements is to use a set of servo-motors connected to each element. For large arrays with fully nonuniform spaced elements, i.e., large number of the movable elements, the computational time (i.e., the number of iterations that are required by the optimization algorithm to converge) becomes a real challenging issue. In addition, an extra time is needed

for mechanical movement of the element positions. Thus, these methods of fully nonuniform spaced arrays were not widely used in practice.

To overcome these problems and make them more amendable in practice, some researchers, for example, see [22–25], have found that the required nulls can be introduced by controlling the positions of only selected elements rather than controlling the positions of all elements.

3.1 Fully nonuniform spaced array

Generally, the optimization parameters of the mechanically nonuniformly spaced arrays can be chosen by either in terms of inter-element spacing between successive elements or in terms of absolute positions of the elements from the center of the array. These two structures are illustrated in **Figure 16**. Choosing the second structure in the optimization process may cause the element positions to overlap. The overlapping between any two or more elements may help to remove (or turn it off) some redundant elements for the thinning arrays. Thus, the second structure is considered in the present work.

The far-field radiation pattern of an array consisting of N isotropic mechanically movable elements that are arranged in nonuniform locations x_n according to the second structure (see **Figure 16**), can be written by [26]

$$AF(u) = 2 \sum_{n=1}^{N/2} a_n \cos(kx_n u) \quad (8)$$

where N is assumed an even number, and a_n is the electronic weighting of the array elements which is chosen to be constant or uniform in this method. In order to introduce the required nulls and at the same time reducing the sidelobe level in the array pattern of (8), the following cost function is used [26]

$$CostFunction = 10 \log_{10} \left[\max(|AF(u)|^2) + \sum_{i=1}^I |AF(u_{i_{upperbound}} \& u_{i_{lowerbound}})| \right] \quad (9)$$

where $\lambda/Nd \leq u \leq 1$, and $i = 1, 2, \dots, I$. Note that λ/Nd represents the angular location of the first null in the array pattern and I represents the total number of the steered nulls. To control the width of the produced nulls, some constraints on the upper and lower bounds are imposed in (9). Note that the first term in (9) corresponds to the peak sidelobe level and the second term corresponds to the required nulls with pre-specified width.

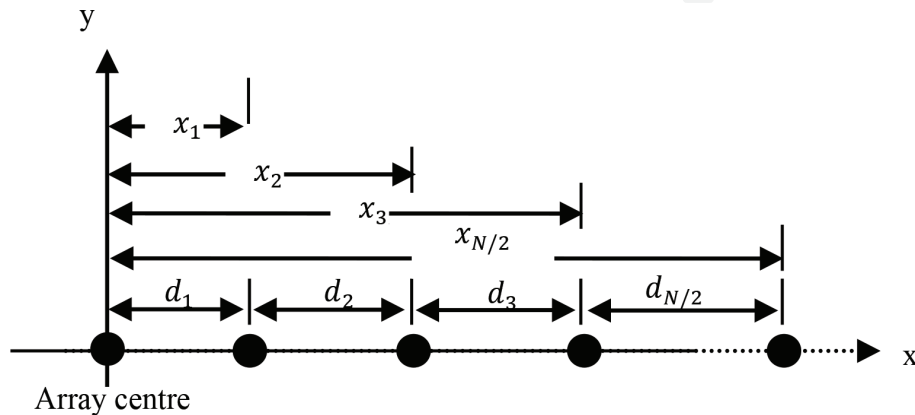


Figure 16. Array structures in terms of Inter-element spacing and absolute locations from the array center [26].

As can be seen from (8) and (9), the positions of all elements are needed to be moveable to meet the required goals. To perform such movements, a number of servo-motors equal to N are needed. These fully mechanical nonuniform spaced arrays may perform very well against the interfering signals that originate from fixed and pre-defined directions. However, such arrays may become impractical in the case of unknown direction or in the case of moving interfering signal (i.e., its incoming direction is changing repeatedly). This means that the designer needs to continuously and quickly recalculate the new location of all elements before the interfering signal can change its direction. Redesigning the array in a very short time interval is really a challenging problem. One effective and simple solution to this important problem is addressed and proposed in [26].

3.2 The results

Each wide null at the desired direction is generated by forming two adjacent nulls with a small spacing equal to $u = 0.02$ around the interfering directions. The effectiveness of the simplified null steering array [26] compared to the fully nonuniform spaced array has been illustrated by the design of 30 elements linear array with the main beam directed toward the broadside. The smoothing, elite sample selection and population parameters of the optimization algorithm are chosen to be 0.7, 0.1, and 100, respectively [26].

In the first example, the fully nonuniform spaced array where all of its elements are made movable is considered. It is assumed that the width of the required nulls in the optimized array are from 0.42 to 0.44 and from 0.61 to 0.63 in u -space, while the depth of these two nulls is chosen to be -40 dB. Also, it is assumed that the electronic amplitude and phase excitations for all elements in the considered array are uniform, i.e., $a_n = 1$. Note, to maintain the overall array length unchanged, the first and the last array elements' locations are fixed. Moreover, in all cases, the cost function represented in (9) is chosen such that it minimizes the output power at the intended null direction(s), i.e., it contains only the second term while the first term which is responsible for sidelobe reduction is omitted. **Figure 17** shows the radiation pattern of the fully nonuniform spaced array. For comparison, the radiation pattern of the fully uniform spaced array is also shown in **Figure 17**(right). From this figure, it can be seen that the capability of the fully nonuniform spaced array for accomplishing the required nulls is more than satisfactory. This is mainly due to the availability of many degrees of freedom. On the other hand, the sidelobe structure has generally increased by few dBs. This is mainly due to the considered cost function as mentioned earlier. The optimized location of all elements with respect to that of the uniformly spaced array is shown in **Figure 17**(left). Note that, as

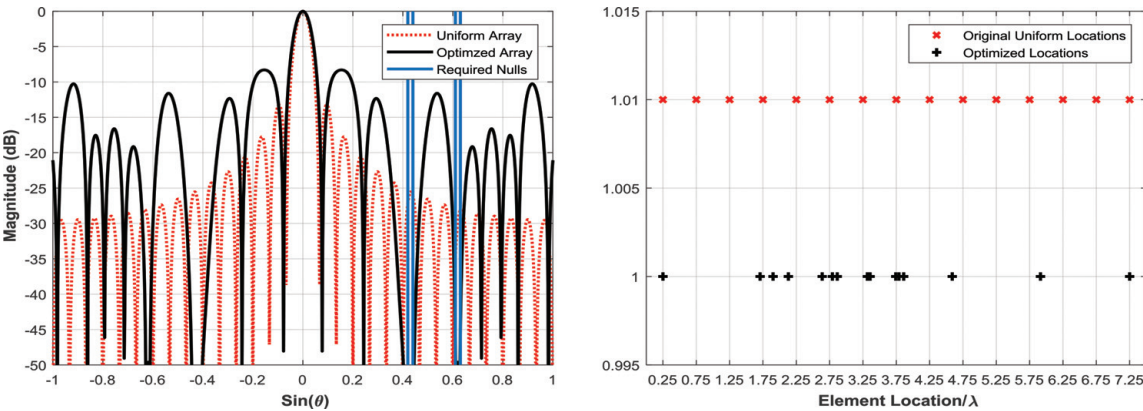


Figure 17.
Results of fully uniform and nonuniform spaced arrays for $N = 30$ elements, and two wide nulls.

mentioned earlier, many elements have moved by more than a wavelength, and many of the new locations are overlapped with the formerly adjacent ones. The overlapping may be exploited in the array thinning, while the elements that are located closer than a half wavelength may result in a high mutual coupling. This mutual coupling could completely deteriorate the nulling capability of such arrays. **Table 1** shows the optimized values of the element locations compared to those of the uniformly spaced array.

Figure 18(left) shows the variation of the cost function, i.e., output power at the desired nulls, with respect to the iteration number in the optimized fully nonuniform spaced array. It can be seen that it takes more than 140 iterations to reach the required depth of -40 dB. **Figure 18**(right) shows the instantaneous

| The Methods | | |
|-------------|---------------------------------|-------------------------------|
| Element # | Original uniformly spaced array | Fully nonuniform spaced array |
| 1 | 0.25 | 0.2500 |
| 2 | 0.75 | 0.7087 |
| 3 | 1.25 | 1.0444 |
| 4 | 1.75 | 1.3522 |
| 5 | 2.25 | 1.9881 |
| 6 | 2.75 | 2.3441 |
| 7 | 3.25 | 2.8279 |
| 8 | 3.75 | 3.1272 |
| 9 | 4.25 | 3.5675 |
| 10 | 4.75 | 4.0763 |
| 11 | 5.25 | 4.5535 |
| 12 | 5.75 | 4.8767 |
| 13 | 6.25 | 5.7395 |
| 14 | 6.75 | 6.5707 |
| 15 | 7.25 | 7.2500 |

The bold values represent the optimized values.

Table 1.
Element locations (in wavelength).

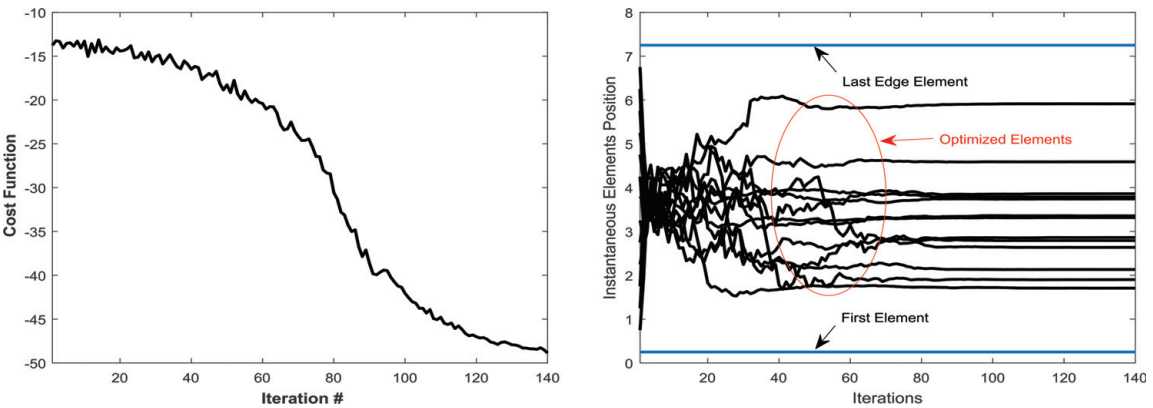


Figure 18.
Convergence speed of the optimizer (left) and the Instantaneous element positions (right).

elements' positions during the optimization process. Note that the initial positions were chosen to start from a uniformly spaced state. Clearly, the computational time that is required by the optimizer to reach the final optimized positions is relatively high since the location of all array elements are made movable. It is shown that the fully nonuniform spaced array performs very well in suppressing the undesired interfering signals, but, at the cost of extra mechanical parts. This problem was efficiently solved in [26] while still maintaining the same performance for interference suppression. More results and discussions can be found in [26].

4. Conclusions

It is shown that the required sidelobe nulling can be accomplished either electronically by controlling the amplitude and/or phase of the excitations of the array elements or mechanically by controlling the positions of all or a small number of the array elements. Each approach has its own advantages and disadvantages. The electronic null steering methods are easy to implement, however, they are associated with some practical problems such as quantization errors which may cause a significant deviation in the desired null directions and finally leads to noticeable performance degradation. On the other hand, the mechanical null steering methods does not need digital attenuator and/or digital phase shifters, thus, they are free from any quantization errors. Instead, each array element in the mechanical null steering methods needs a servo-motor to make the element moveable. If all or most of the array elements are required to be movable, then a considerable extra time is needed for mechanical movement of the elements. This represents a real challenging issue in the practice.


To solve these aforementioned problems that were associated with both electronic and mechanical methods of sidelobe nulling, it is proposed to control only some selected elements rather than controlling all of the array elements that were required for array pattern reconfiguration. The number of the array elements, the operating frequency, and the accuracy at which the desired pattern is needed influence the final choice between the two approaches of electronic and mechanical sidelobe nulling.

Author details

Jafar Ramadhan Mohammed* and Khalil H. Sayidmarie
College of Electronic Engineering, Ninevah University, Mosul, Iraq

*Address all correspondence to: jafarram@yahoo.com

IntechOpen

© 2019 The Author(s). Licensee IntechOpen. This chapter is distributed under the terms of the Creative Commons Attribution License (<http://creativecommons.org/licenses/by/3.0>), which permits unrestricted use, distribution, and reproduction in any medium, provided the original work is properly cited. 

References

- [1] Compton RT. Adaptive Antennas. New Jersey: Prentice Hall; 1988
- [2] Van Veen BD, Buckley KM. Beamforming: A versatile approach to spatial filtering. *IEEE ASSP Magazine*. 1988;5(2):4-24
- [3] Haupt RL. Phase-only adaptive nulling with a genetic algorithm. *IEEE Transactions on Antennas and Propagation*. 1997;45(6):1009-1015
- [4] Rocca P, Mailloux RJ, Toso G. Ga-based optimization of irregular subarray layouts for wideband phased arrays design. *IEEE Antennas and Wireless Propagation Letters*. 2015;14:131-134
- [5] Steyskal H, Shore RA, Haupt RL. Methods for null control and their effects on the radiation pattern. *IEEE Transactions on Antennas and Propagation*. 1986;34:404-409
- [6] Rahman SU, Qunsheng C, Muhammad M, Hisham K. Analysis for linear antenna array for minimum sidelobe level, half power beamwidth, and null control using PSO. *Journal of Microwaves, Optoelectronics and Electromagnetic Applications*. 2017;16(2):577-591
- [7] Khodier MM, Christodoulou CG. Linear array geometry synthesis with minimum sidelobe level and null control using particle swarm optimization. *IEEE Transactions on Antennas and Propagation*. 2005;53(8):2674-2679
- [8] Trastoy A, Ares F, Moreno E. Phase-only control of antenna sum and shaped patterns through null perturbation. *IEEE Antennas and Propagation Magazine*. 2001;43(6):45-54
- [9] Smith SK, Bregains JC, Melde KL, Ares F. A comparison of optimization techniques for power patterns with low sidelobes generated by linear arrays with efficient excitation distribution. *Microwave and Optical Technology Letters*. 2005;45(1):57-60
- [10] Prerna S, Ashwin K. Ant Lion Optimization algorithm to control sidelobe level and null depths in linear antenna arrays. *AEU - International Journal of Electronics and Communications*. 2016;70(9):1339-1349
- [11] Gopi R, Durbadal M, Rajib K, Sakti PG. Directivity maximization and optimal far-field pattern of time modulated linear antenna arrays using evolutionary algorithms. *AEU - International Journal of Electronics and Communications*. 2015;69(12):1800-1809
- [12] Banerjee S, Mandal D. Array pattern optimization for a steerable circular isotropic antenna array using the firefly algorithm. *Journal of Computational Electronics*. 2017;16(3):952-976
- [13] Faridani M, Ghalamkari B. Four-element lens array antenna for advanced point-to-(multi)point high-bandwidth wireless communication. *Journal of Computational Electronics*. 2018;17(3):1082-1089
- [14] Mohammed JR, Sayidmarie KH. A new technique for obtaining wide-angular nulling in the sum and difference patterns of monopulse antenna. *IEEE Antennas and Wireless Propagation Letters*. 2012;11:1242-1245
- [15] Mohammed JR. Phased array antenna with ultra-low sidelobes. *Electronics Letters*. 2013;49(17):1055-1056
- [16] Mohammed JR. A new antenna array pattern synthesis method with sidelobe control. *International Journal of Telecommunication, Electronics, and*

Computer Engineering. 2018;**10**(3): 31-36

Microwaves, Antennas and Propagation. 2011;**5**(2):127-135

[17] Mohammed JR, Sayidmarie KH. Null steering method by controlling two elements. IET Microwaves, Antennas and Propagation. 2014;**8**(15):1348-1355

[25] Basbug S. Design and synthesis of antenna array with movable elements along semicircular paths. IEEE Antennas and Wireless Propagation Letters. 2017; **16**:3059-3062

[18] Mohammed JR, Sayidmarie KH. Sidelobe cancellation for uniformly excited planar array antennas by controlling the side elements. IEEE Antennas and Wireless Propagation Letters. 2014;**13**:987-990

[26] Mohammed JR. Obtaining wide steered nulls in linear array patterns by controlling the locations of two edge elements. AEU - International Journal of Electronics and Communications. Accepted for publication

[19] Mohammed JR, Sayidmarie KH. Synthesizing asymmetric side lobe pattern with steered nulling in nonuniformly excited linear arrays by controlling edge elements. International Journal of Antennas and Propagation. 24 May 2017;**2017**:1-7. Article ID: 9293031. <https://doi.org/10.1155/2017/9293031>

[27] Mohammed JR, Sayidmarie KH. Performance evaluation of the adaptive sidelobe canceller system with various auxiliary configurations. International Journal of Electronics and Communications (AEÜ). 2017;**80**: 179-185

[20] Mohammed JR. Optimal null steering method in uniformly excited equally spaced linear arrays by optimizing two edge elements. Electronics Letters. 2017;**53**(13):835-837

[28] Mohammed JR, Sayidmarie KH. Planar array with optimized perimeter elements. In: 2018 Advances in Wireless and Optical Communications (RTUWO); 15–16 November, 2018; Riga, Latvia. Accepted for presentation

[21] Mohammed JR. Element selection for optimized multi-wide nulls in almost uniformly excited arrays. IEEE Antennas and Wireless Propagation Letters. 2018;**17**(4):629-632

[29] Mohammed JR, Sayidmarie KH. Sensitivity of the adaptive nulling to random errors in amplitude and phase excitations in array elements. International Journal of Telecommunication, Electronics, and Computer Engineering. 2018;**10**(1): 51-56

[22] Mohammed JR. Thinning a subset of selected elements for null steering using binary genetic algorithm. Progress in Electromagnetics Research M. 2018;**67**: 147-157

[30] Sayidmarie KH, Mohammed JR. Performance of a wide angle and wideband nulling method for phased arrays. Progress in Electromagnetics Research M. 2013;**33**:239-249

[23] Hejres J. Null steering in phased arrays by controlling the positions of selected elements. IEEE Transactions on Antennas and Propagation. 2004;**52**(11): 2891-2895

[24] Tokan F, Güneş F. Interference suppression by optimizing the positions of selected elements using generalized pattern search algorithm. IET